RAE-1 ligands for the NKG2D receptor are regulated by STING-dependent DNA sensor pathways in lymphoma

Adeline R Lam[#1,2], **Nina Le Bert**[#1], **Samantha SW Ho**[1], **Yu J Shen**[1,2], **Li FM Tang**[1], **Gordon M Xiong**[1], **John L Croxford**[1], **Christine X Koo**[1,2,3,4], **Ken J Ishii**[3,4], **Shizuo Akira**[5], **David H Raulet**[#6], and **Stephan Gasser**[#1,2,§]

[1]Immunology Programme and Department of Microbiology, Centre for Life Sciences, National University of Singapore, 117456, Singapore

[2]NUS Graduate School for Integrative Sciences and Engineering, National University of Singapore, 117597 Singapore

[3]Laboratory of Adjuvant Innovation, National Institute of Biomedical Innovation (NIBIO), 7-6-8 Saito-Asagi, Ibaraki, Osaka, Japan

[4]Laboratory of Vaccine Science, WPI Immunology Frontier Research Center (iFREC), Osaka University, 3-1 Yamadaoka, Suita, Osaka, Japan

[5]WPI Immunology Frontier Research Center (iFREC), Osaka University, 3-1 Yamadaoka, Suita, Osaka, Japan

[6]Department of Molecular and Cell Biology and Cancer Research Laboratory, University of California, Berkeley, CA 94720-3200, USA.

[#] These authors contributed equally to this work.

Abstract

The immunoreceptor NKG2D originally identified in natural killer cells recognizes ligands that are upregulated on tumor cells. Expression of NKG2D ligands (NKG2DLs) is activated by the DNA damage response (DDR) which is often activated constitutively in cancer cells, revealing them to natural killer cells as a mechanism of immunosurveillance. Here we report that the induction of retinoic acid early transcript 1 (RAE1) ligands for NKG2D by the DDR relies on a STING-dependent DNA sensor pathway involving the effector molecules TBK1 and IRF3. Cytosolic DNA was detected in lymphoma cell lines which express RAE1 and its occurrence required activation of the DDR. Transfection of DNA into ligand-negative cells was sufficient to induce RAE1 expression. Irf3$^{+/-}$;Eμ-Myc mice expressed lower levels of RAE1 on tumor cells and showed a reduced survival rate compared to Irf3$^{+/+}$;Eμ-Myc mice. Taken together, our results suggest that genomic damage in tumor cells leads to activation of STING-dependent DNA sensor pathways, thereby activating RAE1 and enabling tumor immunosurveillance.

§ Correspondence and requests for materials should be addressed to S.G. (micsg@nus.edu.sg). Immunology Programme, Department of Microbiology, National University of Singapore, 117456, Singapore..

Keywords

Innate immunity; NK cells; DNA sensor; DNA damage response; NKG2D

INTRODUCTION

The NKG2D system is an arm of innate immune recognition, which is important in the context of both cancer and infection (1-3). Transformed and infected cells increase the expression of NKG2DLs. Engagement of the NKG2D receptor on natural killer (NK) cells and certain T cells stimulates their effector functions, which aid in tumor control (4, 5). Recently, we elucidated a principle mechanism that induces NKG2DLs in cancer cells: the DDR (6). DNA damage upregulates the expression of numerous NKG2DLs, including different retinoic acid early transcript (RAE1) isoforms and mouse UL16-binding protein-like transcript 1 (MULT1) in mouse cells. The DDR molecules ATR (ataxia-telangiectasia and Rad3-related), ATM (ataxia-telangiectasia mutated homolog) and CHK1 (checkpoint kinase-1 homolog) are required for expression of NKG2DLs in response to DNA damage and the constitutive expression of NKG2DLs in some tumor cell lines (6). Additional effector molecules of the DDR required for mouse NKG2DL expression have not been identified.

Optimal immune responses to autologous cells often require the presence of pathogen- and damage-associated molecular patterns. Pattern recognition receptors (PRR) that recognize self-molecules, such as DNA, have been suggested to play a role in cancer (7). Recently identified candidate cytosolic DNA sensors include ZBP1/DAI (Z-DNA binding protein 1) and Rig-I (retinoic acid inducible gene I) (8). Upon recognizing DNA these sensors activate stimulator of interferon genes (STING), TANK-binding kinase-1 (TBK1) and/or the related IKK-related kinase epsilon (IKKε) (9). Activated TBK1 and IKKε directly phosphorylate interferon regulatory factor-3 (IRF3), which subsequently undergoes dimerization and translocation into the nucleus (10). Nuclear IRF3 induces the expression of target genes including interferon beta (*Infb*) and chemokine C-C motif ligand-5 (*Ccl5*) (11).

Expression of the proto-oncogene *c-MYC* is deregulated in 70% of human cancers. Overexpression of *c-MYC* induces DNA damage and the DDR, which was suggested to act as a barrier against tumor development in premalignant cells (12, 13). In Eμ-*Myc* transgenic mice, c-*Myc* expression is driven by the IgH Eμ enhancer leading to precursor-B cell malignancies similar to human Burkitt's lymphoma (14, 15). The tumor suppressors that prevent the development of *c-Myc* expressing premalignant cells have not been well characterized.

In the present study, we show that the DDR leads to the presence of cytosolic DNA and activation of IRF3 in lymphoma cell lines. The induction of RAE1 ligands by the DDR depended on IRF3. Transfection of cells with cytosolic DNA induced the expression of RAE1 molecules. Tumors in $Irf3^{+/-}$;Eμ-*Myc* mice expressed lower levels of RAE1 and developed lymphoma earlier resulting in a shortened life span when compared to $Irf3^{+/+}$;Eμ-*Myc* mice. Taken together, these findings link genotoxic stress to cytosolic DNA sensor signaling pathways and the induction of RAE1 in lymphoma cell lines.

MATERIAL and METHODS

Cells

BC2 (a kind gift by Dr. Corcoran) and EμM1 cells were derived from Eμ-*Myc* mice (16). Yac-1 cells were purchased from ATCC. Cells were cultured in RPMI-1660 medium (Invitrogen) with 10% FCS (Hyclone), 50 μM 2-mercaptoethanol, 100 μM asparagine, 2 mM glutamine (Sigma), 1% pen/strep (Invitrogen) and 1/1000 plasmocin (Invivogen).

EμM1, mouse embryonic fibroblasts (MEFs) and tumor cells in Eμ-*Myc* mice (C57BL/6) express RAE1βδ and/or RAE1ε. BC2 (C57BL6//129) and Yac-1 (A/Sn) express RAE1α, RAE1β, RAE1γ and RAE1δ.

Reagents

Aphidicolin, caffeine, CGK733, cytosine β-D-arabinofuranoside hydrochloride (Ara-C), TransFectin, DMSO, Poly G:C, Poly A:U and Poly I:C were purchased from Sigma. KU55933 and VE-821 were obtained from Tocris Bioscience or Axon Medchem. ODN1585, ODN1668 control (ssDNA), and LPS were purchased from Invivogen. DNA was conjugated to Alexa-488 using the Ulysis-labelling kit according to manufacturer's instructions (Invitrogen).

Constructs and Transduction

Irf3, *Tbk1, Ikke, Sting*-HA, *Irf3-Egfp* and *Irf3A7-Egfp* were subcloned into the pMSCV2.2-IRES-*Gfp* vector (gift of Dr. Sha, University of California, Berkeley). Wild-type (WT) and mutant *Sting* fibroblasts were kindly provided by Dr. Vance (University of California, Berkeley). Retroviral supernatants were generated as described in (17). shRNA constructs were cloned into the MSCV/LTRmiR30-PIG vector (Open Biosystems) (See supplementary data).

Quantitative Real-time RT-PCR

Performed as described in (6).

Native PAGE Gel Electrophoresis

Performed as described in (18).

Western Blotting

Whole cell extracts were electrophoresed in 10% or 4-20% SDS-PAGE gels and blotted onto nitrocellulose membranes (BioRad). Antibodies against IRF3, IRF3pSer396, TBK1, TBK1pSer172, ATM, ATMpSer1981 (Cell Signaling Technology), BCL2L12 (clone E-13, Santa Cruz) and GAPDH (Sigma) and horseradish peroxidase-coupled second stage reagents were used (Thermo). Blots were exposed on X-ray film (Fuji); densitometry analysis was performed using ImageJ-1.46r.

Flow Cytometry

The following antibodies were used: pan-RAE1, RAE1αβγ, RAE1βδ, RAE1ε (R&D Systems), B220-PerCP, IgM-APC, CD16/CD32, MHC class II (eBioscience), rabbit-anti-phospho-IRF3-Ser396 or rabbit-anti-phospho-TBK1-Ser172 (Cell Signaling Technology) and rat IgG-APC (eBioscience) or rabbit IgG-Alexa-488 (Invitrogen). 1 μg/ml propidium iodide (PI) was added to all stainings and PI negative cells are shown. For intracellular staining, cells were fixed according to the manufacturer's protocol. Some cells were treated with 2 U/μl λ-phosphatase (NEB) at 37°C for 90 min before staining. Stained cells were analyzed using FACSCalibur and FlowJo. 8.8.7. (Treestar). BrdU incorporation analysis were performed as described (19).

Microscopy

Cells were fixed and stained for DNA according to manufacturer's instructions (Millipore). A detailed protocol is provided in the supplementary data.

CD107a Degranulation Assay and *In Vitro* NK cell Stimulation

Performed as described in (4) and (20).

Statistical Analyses

Groups were compared using 2-tailed unpaired *t*-tests (Prism, 5.0c, GraphPad). Survival was represented by Kaplan-Meier curves and statistical analysis was performed with the log rank Mantel-Cox Test.

RESULTS

IRF3 is Necessary for RAE1 Expression in Response to DNA Damage

IRF3 has previously been shown to be activated in response to DNA damage (21, 22). We therefore investigated the role of IRF3 in the expression of NKG2DLs in cells exposed to DNA damaging agents. Phosphorylation of serine 396 (S388 of mouse IRF3) has been shown to be critical for the activation of IRF3 (23). Phosphorylation of IRF3S388 increased after treatment with DDR-inducing agents Ara-C or aphidicolin, although not to the same degree as lipopolysaccharides (LPS), a known inducer of IRF3 (Fig. 1A-B, S1A) (24). The late kinetics of IRFS388 phosphorylation were similar to kinetics previously observed for DNA damage-induced upregulation of NKG2DLs (6). Notably, treatment of BC2 cells with Ara-C also induced activated IRF3 characterized by nuclear translocation of endogenous IRF3 (Fig. 1C) and overexpressed chimeric IRF3-GFP (Fig. 1D-E) consistent with previous reports (21, 22). No nuclear translocation was observed with a mutant form of IRF3 (IRF3A7-GFP) that is unable to be activated (Fig. 1D-E). Treatment of BC2 cells with Ara-C or aphidicolin induced expression of several IRF3 target genes to a similar or greater extent than Poly I:C, an established IRF3 activator, suggesting that IRF3 is transcriptionally active in response to DNA damage (Fig. 1F-G).

To test if IRF3 is required for DDR-mediated upregulation of NKG2DLs, we transduced BC2 cells with an *Irf3*-specific shRNA (Fig. S1B). Compared to control shRNA, *Irf3*-

specific shRNA significantly inhibited the upregulation of RAE1 ligands of NKG2D, but not MHC class II, in response to Ara-C (Fig. 1H).

Bimodal expression of RAE1 is likely to reflect specific activation of the DDR in S-phase of the cell cycle. No consistent effects were observed for the NKG2DLs MULT-1 and H60 suggesting that upregulation of MULT-1 in response to DNA damage requires additional signals.

To address if IRF3-induced RAE1 expression renders cells more sensitive to NK cell-mediated lysis, *Irf3*-specific and control shRNA-transduced cells were cultured with IL-2-activated NK cells. BC2 cells transduced with *Irf3*-specificshRNA were less sensitive to NK cell-mediated cytotoxicity in response to Ara-C treatment than control shRNA-transduced BC2 cells (Fig. 1I). The sensitivity of *Irf3*-shRNA-transduced BC2 cells was similar to control shRNA-transduced BC2 cells treated with Ara-C in the presence of NKG2D-blocking antibodies, suggesting that decreased lysis of *Irf3*-shRNA-transduced cells was due to reduced RAE1 expression.

IRF3 is Required for Constitutive RAE1 Expression in Yac-1 cells

The DDR is constitutively activated in many tumor cell lines and precancerous lesions (25). In agreement, phosphorylation of IRF3S388 was detected in EμM1 cells and Yac-1 lymphoma cells (Fig. 2A). Endogenous IRF3 (Fig. 2B) and exogenous chimeric IRF3-GFP (Fig. 2C) were partially localized to the nucleus, indicating that a subset of IRF3 is activated in EμM1 and Yac-1 cells. In contrast, IRF3A7 exhibited exclusively cytosolic localization in Yac-1 cells. Inhibition of IRF3 expression in EμM1 and Yac-1 cells by shRNA decreased the expression of IRF3 target genes (Fig. 2D-E), *Raet1* transcripts (Fig. S1C) and RAE1 cell surface levels (Fig. 2F). Mouse strains were found to express different RAE-1 isoforms and the cell lines used in this study vary in their genetic background (see material and methods) (26). The incomplete reduction of cell surface RAE1 expression by *Irf3*-specific shRNAs may reflect incomplete turnover of preformed RAE1 or incomplete knockdown of IRF3 (Fig. S1B).

TBK1 is Necessary for RAE1 Expression in Response to DNA Damage

IRF3 is activated by the IKK-related serine/threonine kinases TBK1 and IKKε (10). We therefore tested whether TBK1 was phosphorylated in response to DNA damage. Similar to results with IRF3, substantial phosphorylation of TBK1 on serine 172 was detected after 15 hours of treatment with Ara-C or aphidicolin, although the activation was weaker than TBK1 phosphorylation in response to LPS (Fig. 3A-B, S2A). No *Ikke* expression was detected in BC2 cells (data not shown).

Transduction of BC2 cells with the TBK1 inhibitor *Sike* caused substantial reduction in RAE1 expression in response to DNA damage (Fig. 3C). Similarly, BC2 cells transduced with *Tbk1*-specific shRNA expressed less transcripts and RAE1 at the cell surface in response to Ara-C (Fig. 3D, S2B). *Tbk1- and Ikke*-deficient MEFs failed to upregulate RAE1 in response to Ara-C (Fig. 3E). Genetic reconstitution of *Tbk1$^{-/-}$Ikke$^{-/-}$* MEFs with *Tbk1* or *Ikkε* was sufficient to induce RAE1 expression on a fraction of cells and to restore

the capacity of cells to upregulate RAE1 in response to Ara-C (Fig. 3E). The induction of RAE1 in untreated cells is likely a consequence of overexpression of *Tbk1* or *Ikkε*, which has been shown to result in unregulated activation of the pathway (27). In summary, the data suggest that TBK1 is required for induction of RAE1 in response to DNA damage in BC2 cells.

TBK1 is Required for Constitutive RAE1 Expression

Similarly to IRF3, constitutive phosphorylation of TBK1S172 was detected in Yac-1 and EµM1 cells (Fig. 3F). Transduction of *Sike* into Yac-1 cells caused reductions in RAE1 levels (Fig. 3G). Expression of a *Tbk1*-specific shRNA in Yac-1 cells decreased the amount of *Raet1* transcripts, and a significant but less complete reduction in RAE1 at the cell surface (Fig. 3H-I). No *Ikke* transcripts were detected in Yac-1 cells (not shown).

Phosphorylation of IRF3 and TBK1 Depends on the DDR

Treatment of cells with Ara-C results in DNA breaks and the activation of ATR and ATM (28). To address the role of ATM and ATR in the activation of TBK1 and IRF3, we blocked ATM and ATR function with different chemical inhibitors. Attempts to efficiently block both ATM and ATR by shRNA were not successful. Induction of RAE1 expression in BC2 cells by Ara-C was inhibited by the combined treatment of cells with ATM and ATR inhibitors (Fig. 4A, S3A). Inhibition of ATM and ATR also impaired TBK1 and IRF3 phosphorylation (Fig. 4B-C, S3B) and nuclear localization of chimeric IRF3-GFP (Fig. 1D-E) in Ara-C-treated BC2 cells. The effects of ATM or ATR inhibition on RAE1 expression and phosphorylation of TBK1 and IRF3 were less pronounced suggesting that ATM and ATR act redundantly (Fig. 4A-C).

Inhibition of ATR impaired constitutive RAE1 expression and phosphorylation of TBK1 and IRF3 in Yac-1 cells (Fig. 4D-E, S3C-D). Nuclear localization of IRF3-GFP in Yac-1 cells was also suppressed by inhibition of ATR and ATM (Fig. 4F). Thus, activation of TBK1 and IRF3 in Yac-1 cells depends on ATR suggesting that DNA damage, which preferentially activates ATR (29), is present in Yac-1 cells.

Accumulation of Cytosolic DNA Depends on the DDR

Recognition of cytosolic DNA by DNA sensors activates TBK1 and IRF3 (8). To test whether DNA damage leads to appearance of cytosolic DNA, we stained cells with antibodies specific for single-stranded (ss)DNA or double-stranded (ds)DNA (Fig. S4A). The specificity of the DNA-staining was verified by pretreating cells with S1 nuclease to degrade ssDNA or DNase I to digest dsDNA before staining (Fig. S4B-C). All cells were treated with RNase before staining. Strikingly, we found that ssDNA and dsDNA occurred in the cytosol of BC2 cells in response to Ara-C treatment and cytosolic DNA was constitutively present in Yac-1 cells (Fig. 5A-B). To substantiate the presence of DNA in the cytosol of cells, we stained BC2 cells with PicoGreen, a vital dsDNA-specific dye (Fig. S4D). In agreement with the dsDNA-specific antibody stainings, PicoGreen staining showed the presence of cytosolic dsDNA in Yac-1 and Ara-C-treated BC2 cells (Fig. 5C, S5A-B). To exclude the possibility that cytosolic DNA represents mitochondrial DNA, we co-stained cells with mitochondria-specific MitoTracker dye or the mitochondrial marker COX-IV

(Fig. 5C, S4-6). As Ara-C disrupted MitoTracker staining, we treated BC2 cells with aphidicolin, an inhibitor of nuclear DNA synthesis that activates the DDR but does not affect replication of mitochondrial DNA (Fig. 5C, S4D) (30). Three-dimensional rendering of confocal microscopy data showed that most cytosolic DNA is present outside of mitochondria in Yac-1 and Ara-C-treated BC2 cells (Fig. 5C, S4D, S5).

To test if the DDR influences the occurrence of cytosolic DNA, we pretreated BC2 cells with ATM and/or ATR inhibitors before treatment with Ara-C. Blocking of ATM and ATR prevented appearance of cytosolic DNA in response to Ara-C (Fig. 5A, S6A). Strikingly, cytosolic DNA present in Yac-1 cells disappeared after inhibition of ATR for 14 hours (Fig. 5B, S6B). Inhibition of ATM had a less pronounced effect on the occurrence of cytosolic DNA in agreement with effects observed on RAE1 expression and phosphorylation of IRF3 and TBK1 (Fig. 5A-B). However, the disappearance of cytosolic DNA in response to inhibition of ATM and ATR did not abrogate RAE1 expression in Yac-1 cells suggesting that RAE1 expression is regulated by additional pathways (26). In summary, our data suggest that appearance of cytosolic DNA depends on the DDR and is rapidly turned over.

Cytosolic DNA Induces RAE1 Expression

To test whether cytosolic DNA induces RAE1 expression in BC2 cells we transfected cells with Alexa-488-labelled plasmid DNA, genomic DNA or ssDNA. We were unable to purify sufficient quantities of cytosolic DNA to determine whether cytosolic DNA present in Ara-C-treated BC2 cells directly induces RAE1 expression. Alexa-488-positive BC2 cells upregulated expression of RAE1, although to a lesser degree than Ara-C-treated cells (Fig. 6A).

The presence of DNA in the cytosol activates STING-dependent DNA sensors leading to the activation of TBK1 and IRF3 (8). We therefore tested whether STING is necessary for RAE1 expression in cells exposed to genotoxic stress. MEFs harboring a loss-of-function *Sting* mutation failed to upregulate RAE1 in response to Ara-C (Fig. 6B). Reconstitution of *Sting* expression resulted in restored inducibility of RAE1 in the cells. Furthermore, RAE1 induction by Ara-C was impaired in BC2 cells expressing a *Sting*-specific shRNA (Fig. 6C) and *Sting* inhibition in Yac-1 cells resulted in reduced constitutive RAE1 expression (Fig. 6D).

Next, we tested the requirement in RAE1 induction for one candidate STING-dependent DNA sensor, ZBP/DAI, that activates IRF3 (8). Knockdown of *Zbp1/Dai* partly inhibited the upregulation of RAE1αβγ in response to Ara-C, but had little effect on RAE1βδ (Fig. 6C). In contrast, knockdown of ZBP1/DAI modestly inhibited RAE1βδ but not RAE1αβγ expression in Yac-1 cells (Fig. 6D). Inhibition of Rig-I, a RNA sensor that may indirectly mediate responses to cytosolic DNA, had no effect on RAE1 expression in BC2 or Yac-1 cells (Fig. 6C D). Hence, DNA sensors other than ZBP1/DAI are likely to participate in inducing RAE1 expression in response to DNA damage, in line with other evidence suggesting the existence of DNA sensors that act redundantly (31). Taken together, these data suggest that cytosolic DNA sensor pathways regulate RAE1 expression in cells exposed to DNA damage.

IRF3 Regulates RAE1 Expression in B-Cell Lymphomas of Eµ-*Myc* mice

To address if IRF3 regulates RAE1 expression in lymphomas, *Irf3*-deficient mice were bred to mice overexpressing c-*Myc* under the control of Ig heavy chain enhancer region (Eµ), analogous to human Burkitt lymphoma (32). Spontaneous B220^{low} B-cell lymphomas develop by 15-20 weeks of age and the progression of lymphomas is accelerated in NKG2D$^{-/-}$;Eµ-*Myc* mice (4, 33). Tumor cells in Eµ-*Myc* mice express phosphorylated ATM (ATMpS1981) (Fig. 7A) (34). Staining of tumor cells with a dsDNA-specific antibody revealed the presence of cytosolic dsDNA in B220^{low} tumor cells, but not normal B220$^+$ B-cells (Fig. 7B). The accumulation of cytosolic DNA was strictly dependent on the DDR as administration of the ATM inhibitor KU55933 resulted in reduced levels of cytosolic dsDNA (Fig. 7C). *Irf3*$^{+/-}$;Eµ-*Myc* mice (median survival=62 days) experienced a significantly reduced survival rate compared to *Irf3*$^{+/+}$;Eµ-*Myc* mice (median survival=116 days) (Fig. 7D). We were not able to generate *Irf3*$^{-/-}$;Eµ-*Myc* mice because *Irf3*$^{+/-}$;Eµ-*Myc* mice failed to breed. Heterozygosity of *Irf3* in Eµ-*Myc* mice resulted in 2.5-fold decrease of IRF3 levels and reduced expression of IRF3 target genes in splenic B-cell lymphomas when compared to *Irf3*$^{+/+}$;Eµ-*Myc* mice, suggesting that cytosolic DNA in lymphomas activates IRF3 (Fig. 7A, E). Importantly, reduced levels of IRF3 in lymphomas impaired RAE1ε expression, the only RAE1 family member detected in Eµ-*Myc* tumor cells (Fig. 7F) (35).

The null mutation introduced into the *Irf3* allele also resulted in functional inactivation of the neighboring *Bcl2l12* gene, which promotes or suppress tumorigenesis depending on the cellular context (36, 37). However, heterozyogosity of the gene-targeted locus did not result in reduced BCL2L12 levels or changes in the rate of apoptosis or proliferation of lymphomas (Fig. 7A, S7A-B). Overexpression of *Bcl2l12* in BC2 and EµM1 cells, two cell lines derived from Eµ-*Myc* mice, had no effect on RAE1 expression, proliferation or apoptosis (Fig. 7G, S7C-D). We previously found that NK cells and T- cells contribute to immunosurveillance in Eµ-*Myc* mice (34). However, *Irf3*-deficiency had no impact on NK- and T-cell numbers or NK cell activity (Fig. 7H) (38). In summary, our data suggest that RAE1 ligands are regulated by IRF3 in lymphomas of Eµ-*Myc* mice. Interestingly, IRF3 is likely to have additional functions in immunosurveillance as NKG2D-deficiency increases the tumor load of Eµ-*Myc* mice, but has no impact on survival (4).

DISCUSSION

Our previous results provided evidence that the DDR activates immune responses by inducing NKG2DLs (6). Here we show that cytosolic DNA contributes to the induction of RAE1 expression in lymphoma cells in response to DNA damage for the following reasons: 1) Inhibition of the DDR impaired the induction of cytosolic DNA and RAE1 molecules; 2) Transfection of DNA into cells upregulated RAE1 expression; 3) Inhibition of STING, TBK1 or IRF3 impaired RAE1 expression; 4) TBK1 and IRF3 were activated in response to DNA damage in a DDR-dependent manner, and 5) Overexpression of TBK1 or IKKε induced RAE1 expression.

Linking the DDR to STING-initiated pathways is of interest immunologically, because STING is a critical component of a major pathway common to receptors that detect cytosolic DNA and RNA of pathogens (8). Previous studies provided indications that the

DDR induces phosphorylation of IRF3 and that certain TLR agonists induce *Raet1* gene expression in peritoneal macrophages (39), but the linkage of these pathways had not been explored. Much remains to be determined concerning the relation of the DDR and STING pathways. We observed less phosphorylation of IRF3 in response to DNA damage when compared to LPS suggesting that IRF3 translocation and transcriptional activity is differentially regulated in response to DNA damage. Consistent with this possibility, Noyce *et al.* reported that no minimal post-translational modification of IRF3 correlated with its transcriptional activity (40). Of interest was that DNA damage consistently led to lower induction of IFN than Poly I:C. The reduced induction likely reflects the fact that the DDR failed to induce IRF7 activation, which is necessary for efficient transcription of IFN genes.

Cytosolic DNA has been shown to be present in cells upon infection or the uptake of apoptotic cells (8). Our data show the presence of cytosolic DNA in uninfected lymphoma cell lines. An intriguing question is where cytosolic DNA originates from and the mechanism leading to cytosolic DNA in tumor cells. DNA damage is known to induce transcription of retroelements, including transposases, derived from functional endogenous retrovirus present in the genome (41). Alternatively, cytosolic DNA could be generated during DDR-dependent DNA-repair that can result in deletion of genomic DNA.

An important question is the nature of the DNA sensor recognizing the cytosolic DNA. The induction of RAE1 by Ara-C partially relied on ZBP1/DAI. ZBP1/DAI is a candidate sensor that is reported to activate TBK1/IRF3 (18). However, additional TBK1-activating DNA sensors exist since MEFs from *Zbp1*$^{-/-}$-deficient mice mount a normal type-I IFN response to DNA (18, 31). These sensors may be required for constitutive RAE1 expression in Yac-1 cells. Hence, unidentified DNA sensors may play a predominant role in YAC-1 cells, or may function redundantly with ZBP1/DAI, in the induction of RAE1.

NKG2D plays an important role in immunosurveillance of tumors in Eµ-*Myc* mice (4, 42). The accelerated development of lymphoma in *Irf3/Bcl2l12*$^{+/-}$;Eµ-*Myc* mice when compared to NKG2D-deficient mice suggests that IRF3 induces the expression of molecules other than RAE1 ligands important for immunosurveillance or suppression of tumorigenesis. IRF3 and BCL2L12 are known to induce genes implicated in apoptosis (11). However, we observed no differences in the rates of apoptosis or proliferation comparing wild-type and heterozygous tumor cells suggesting that accelerated tumorigenesis of *Irf3/Bcl2l12*$^{+/-}$;Eµ-*Myc* mice is not due to effects of IRF3 or BCL2L12 on apoptosis or proliferation. In summary our data suggest that tumorigenesis leads to accumulation of cytosolic DNA and subsequent activation of an anti-tumor immune response that may partially depend on NKG2D.

Supplementary Material

Refer to Web version on PubMed Central for supplementary material.

Acknowledgments

REFERENCES

1. Raulet D. Roles of the NKG2D immunoreceptor and its ligands. Nat Rev Immunol. 2003; 3:781–90. [PubMed: 14523385]

2. Gasser S, Raulet D. The DNA damage response, immunity and cancer. Semin Cancer Biol. 2006; 16:344–7. [PubMed: 16914325]

3. Gasser S, Raulet DH. The DNA damage response arouses the immune system. Cancer Res. 2006; 66:3959–62. [PubMed: 16618710]

4. Guerra N, Tan Y, Joncker N, Choy A, Gallardo F, Xiong N, et al. NKG2D-Deficient Mice Are Defective in Tumor Surveillance in Models of Spontaneous Malignancy. Immunity. 2008; 28:571–80. [PubMed: 18394936]

5. Raulet DH, Guerra N. Oncogenic stress sensed by the immune system: role of natural killer cell receptors. Nat Rev Immunol. 2009; 9:568–80. [PubMed: 19629084]

6. Gasser S, Orsulic S, Brown EJ, Raulet DH. The DNA damage pathway regulates innate immune system ligands of the NKG2D receptor. Nature. 2005; 436:1186–90. [PubMed: 15995699]

7. Rakoff-Nahoum S, Medzhitov R. Toll-like receptors and cancer. Nat Rev Cancer. 2009; 9:57–63. [PubMed: 19052556]

8. Yanai H, Savitsky D, Tamura T, Taniguchi T. Regulation of the cytosolic DNA-sensing system in innate immunity: a current view. Curr Opin Immunol. 2009; 21:17–22. [PubMed: 19362700]

9. Desmet CJ, Ishii KJ. Nucleic acid sensing at the interface between innate and adaptive immunity in vaccination. Nat Rev Immunol. 2012; 12:479–91. [PubMed: 22728526]

10. Fitzgerald KA, McWhirter SM, Faia KL, Rowe DC, Latz E, Golenbock DT, et al. IKKepsilon and TBK1 are essential components of the IRF3 signaling pathway. Nature immunology. 2003; 4:491–6. [PubMed: 12692549]

11. Taniguchi T, Ogasawara K, Takaoka A, Tanaka N. IRF family of transcription factors as regulators of host defense. Annu Rev Immunol. 2001; 19:623–55. [PubMed: 11244049]

12. Packham G, Cleveland JL. c-Myc and apoptosis. Biochim Biophys Acta. 1995; 1242:11–28. [PubMed: 7626652]

13. Reimann M, Loddenkemper C, Rudolph C, Schildhauer I, Teichmann B, Stein H, et al. The Myc-evoked DNA damage response accounts for treatment resistance in primary lymphomas in vivo. Blood. 2007; 110:2996–3004. [PubMed: 17562874]

14. Wang J, Boxer LM. Regulatory elements in the immunoglobulin heavy chain gene 3′-enhancers induce c-myc deregulation and lymphomagenesis in murine B cells. J Biol Chem. 2005; 280:12766–73. [PubMed: 15687498]

15. Adams JM, Harris AW, Pinkert CA, Corcoran LM, Alexander WS, Cory S, et al. The c-myc oncogene driven by immunoglobulin enhancers induces lymphoid malignancy in transgenic mice. Nature. 1985; 318:533–8. [PubMed: 3906410]

16. Corcoran LM, Tawfilis S, Barlow LJ. Generation of B lymphoma cell lines from knockout mice by transformation in vivo with an Emu-myc transgene. J Immunol Methods. 1999; 228:131–8. [PubMed: 10556550]

17. Diefenbach A, Hsia JK, Hsiung MY, Raulet D. A novel ligand for the NKG2D receptor activates NK cells and macrophages and induces tumor immunity. Eur J Immunol. 2003; 33:381–91. [PubMed: 12645935]

18. Takaoka A, Wang Z, Choi M, Yanai H, Negishi H, Ban T, et al. DAI (DLM-1/ZBP1) is a cytosolic DNA sensor and an activator of innate immune response. Nature. 2007; 448:501–5. [PubMed: 17618271]

19. Croxford JL, Tang ML, Pan MF, Huang CW, Kamran N, Phua CM, et al. ATM-dependent spontaneous regression of early Emu-myc-induced murine B cell leukemia depends on NK and T cells. Blood. 2013

20. Sauer M, Reiners KS, Hansen HP, Engert A, Gasser S, von Strandmann EP. Induction of the DNA damage response by IAP inhibition triggers natural immunity via upregulation of NKG2D ligands in Hodgkin lymphoma in vitro. Biol Chem. 2013; 394:1325–31. [PubMed: 23787466]

21. Kim ST, Lim DS, Canman CE, Kastan MB. Substrate specificities and identification of putative substrates of ATM kinase family members. J Biol Chem. 1999; 274:37538–43. [PubMed: 10608806]

22. Servant MJ, Grandvaux N, Hiscott J. Multiple signaling pathways leading to the activation of interferon regulatory factor 3. Biochem Pharmacol. 2002; 64:985–92. [PubMed: 12213596]

23. Hiscott J, Grandvaux N, Sharma S, Tenoever BR, Servant MJ, Lin R. Convergence of the NF-kappaB and interferon signaling pathways in the regulation of antiviral defense and apoptosis. Ann N Y Acad Sci. 2003; 1010:237–48. [PubMed: 15033728]

24. Stein SC, Falck-Pedersen E. Sensing adenovirus infection: activation of interferon regulatory factor 3 in RAW 264.7 cells. J Virol. 2012; 86:4527–37. [PubMed: 22345436]

25. Bartkova J, Horejsi Z, Koed K, Kramer A, Tort F, Zieger K, et al. DNA damage response as a candidate anti-cancer barrier in early human tumorigenesis. Nature. 2005; 434:864–70. [PubMed: 15829956]

26. Raulet DH, Gasser S, Gowen BG, Deng W, Jung H. Regulation of ligands for the NKG2D activating receptor. Annu Rev Immunol. 2013; 31:413–41. [PubMed: 23298206]

27. Fensterl V, Grotheer D, Berk I, Schlemminger S, Vallbracht A, Dotzauer A. Hepatitis A virus suppresses RIG-I-mediated IRF-3 activation to block induction of beta interferon. J Virol. 2005; 79:10968–77. [PubMed: 16103148]

28. D'Incalci M, Covey JM, Zaharko DS, Kohn KW. DNA alkali-labile sites induced by incorporation of 5-aza-2′-deoxycytidine into DNA of mouse leukemia L1210 cells. Cancer Res. 1985; 45:3197–202. [PubMed: 2408746]

29. Sancar A, Lindsey-Boltz LA, Unsal-Kaccmaz K, Linn S. Molecular mechanisms of mammalian DNA repair and the DNA damage checkpoints. Annu Rev Biochem. 2004; 73:39–85. [PubMed: 15189136]

30. Zimmermann W, Chen SM, Bolden A, Weissbach A. Mitochondrial DNA replication does not involve DNA polymerase alpha. J Biol Chem. 1980; 255:11847–52. [PubMed: 6777385]

31. Ishii K, Kawagoe T, Koyama S, Matsui K, Kumar H, Kawai T, et al. TANK-binding kinase-1 delineates innate and adaptive immune responses to DNA vaccines. Nature. 2008; 451:725–9. [PubMed: 18256672]

32. Adams JM, Gerondakis S, Webb E, Corcoran LM, Cory S. Cellular myc oncogene is altered by chromosome translocation to an immunoglobulin locus in murine plasmacytomas and is rearranged similarly in human Burkitt lymphomas. Proc Natl Acad Sci U S A. 1983; 80:1982–6. [PubMed: 6572957]

33. Harris AW, Pinkert CA, Crawford M, Langdon WY, Brinster RL, Adams JM. The E mu-myc transgenic mouse. A model for high-incidence spontaneous lymphoma and leukemia of early B cells. J Exp Med. 1988; 167:353–71. [PubMed: 3258007]

34. Croxford JL, Tang ML, Pan MF, Huang CW, Kamran N, Phua CM, et al. ATM-dependent spontaneous regression of early Emu-myc-induced murine B-cell leukemia depends on natural killer and T cells. Blood. 2013; 121:2512–21. [PubMed: 23349395]

35. Unni AM, Bondar T, Medzhitov R. Intrinsic sensor of oncogenic transformation induces a signal for innate immunosurveillance. Proc Natl Acad Sci U S A. 2008; 105:1686–91. [PubMed: 18223157]

36. Nakajima A, Nishimura K, Nakaima Y, Oh T, Noguchi S, Taniguchi T, et al. Cell type-dependent proapoptotic role of Bcl2L12 revealed by a mutation concomitant with the disruption of the juxtaposed Irf3 gene. Proc Natl Acad Sci U S A. 2009; 106:12448–52. [PubMed: 19617565]

37. Stegh AH, Kim H, Bachoo RM, Forloney KL, Zhang J, Schulze H, et al. Bcl2L12 inhibits post-mitochondrial apoptosis signaling in glioblastoma. Genes Dev. 2007; 21:98–111. [PubMed: 17210792]

38. Sato M, Suemori H, Hata N, Asagiri M, Ogasawara K, Nakao K, et al. Distinct and essential roles of transcription factors IRF-3 and IRF-7 in response to viruses for IFN-alpha/beta gene induction. Immunity. 2000; 13:539–48. [PubMed: 11070172]

39. Hamerman JA, Ogasawara K, Lanier LL. Cutting edge: Toll-like receptor signaling in macrophages induces ligands for the NKG2D receptor. J Immunol. 2004; 172:2001–5. [PubMed: 14764662]

40. Noyce RS, Collins SE, Mossman KL. Differential modification of interferon regulatory factor 3 following virus particle entry. J Virol. 2009; 83:4013–22. [PubMed: 19211751]

41. Wilkins AS. The enemy within: an epigenetic role of retrotransposons in cancer initiation. BioEssays : news and reviews in molecular, cellular and developmental biology. 2010; 32:856–65.

42. Raulet DH, Guerra N. Oncogenic stress sensed by the immune system: role of natural killer cell receptors. Nat Rev Immunol. 2009; 9:568–80. [PubMed: 19629084]
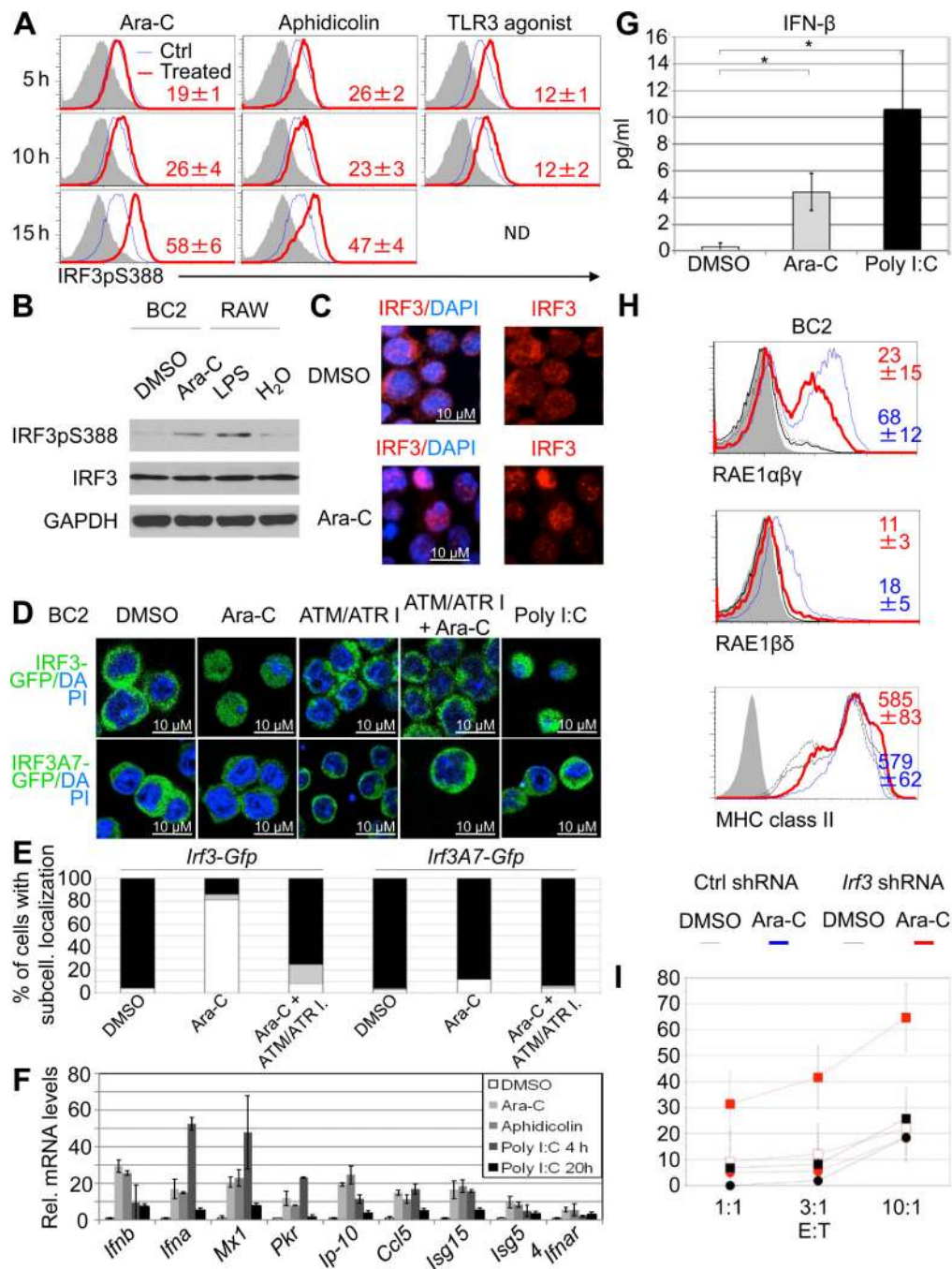
Figure 1. IRF3 is activated and necessary for optimal induction of RAE1 ligands for NKG2D in response to DNA damage

(A) Phosphorylation of IRF3-S388 in BC2 cells treated with 10 μM Ara-C, 4 μM aphidicolin, 1 μg/ml ODN1585 (red line) or DMSO (blue line) was analyzed by intracellular flow cytometry at indicated time points. Filled histograms: isotype staining of Ara-C-treated cells. Mean fluorescence intensity (MFI) ±SD are shown. (B) Phosphorylation of IRF3-S388 after 16 hrs of 10 μM Ara-C or DMSO treatment was analyzed by western-blotting. Raw 264.7 cells were treated with LPS for 4 hrs. (C) Nuclear translocation of endogenous IRF3 (red) in BC2 cells treated with 10 μM Ara-C for 16 hrs and stained for IRF3 in

presence of DAPI (blue). (D-E) BC2 cells expressing *IRF3-Gfp* or *IRF3A7-Gfp* were treated with 10 μM Ara-C, 10 μg/ml Poly I:C or DMSO for 16 hrs. Some cells were pretreated with 10 μM of the ATM/ATR-specific inhibitor CGK733. Localization of IRF3 in DAPI-stained cells was analyzed by fluorescent microscopy (D). Quantification of BC2 cells with nuclear (white bar; >90% nuclear), partial nuclear (grey bar; 10-90% nuclear) and cytosolic (black bar; <10% nuclear) localization of IRF3 (E). (F) BC2 cells were treated with DMSO (white bar), 10 μM Ara-C (light-grey bar), 4 μM aphidicolin (grey bar), 1 μg/ml Poly I:C for 20 hrs (black bar), or 1 μg/ml Poly I:C for 4 hrs (dark-grey bar). Relative mRNA levels of IRF3 target genes were measured by qRT-PCR. Means ±SD of 3 independent experiments normalized to DMSO-treated cells are shown. (G) Levels of IFN-β in supernatants of 0.75×10^6 BC2 cells/ml treated with DMSO, 10 μM Ara-C or 1 μg/ml Poly I:C for 24 hrs were determined by ELISA. *p<0.05. (H) RAE1 expression in *Irf3*-specific (red line) or control (blue line) shRNA-transduced BC2 cells, which were cultured for 5 days in puromycin before treatment with 10 μM Ara-C for 16 hrs. DMSO-treated *Irf3* (dashed line) or control (dotted line) shRNA-transduced cells are also shown. Filled histograms: isotype staining of Ara-C-treated cells. MFI ±SD are indicated. (I) IL-2-activated NK cells were co-cultured with *Irf3*-specific (circles) or control shRNA-transduced (squares) BC2 cells in presence of NKG2D-blocking antibodies (open symbols) or IgG2a isotype control antibodies (filled symbols) and treated with 10 μM Ara-C (red) or DMSO (black) for 16 hrs. The effector (E) to target (T) ratio is indicated. Results ±SD of 3 independent experiments are shown.
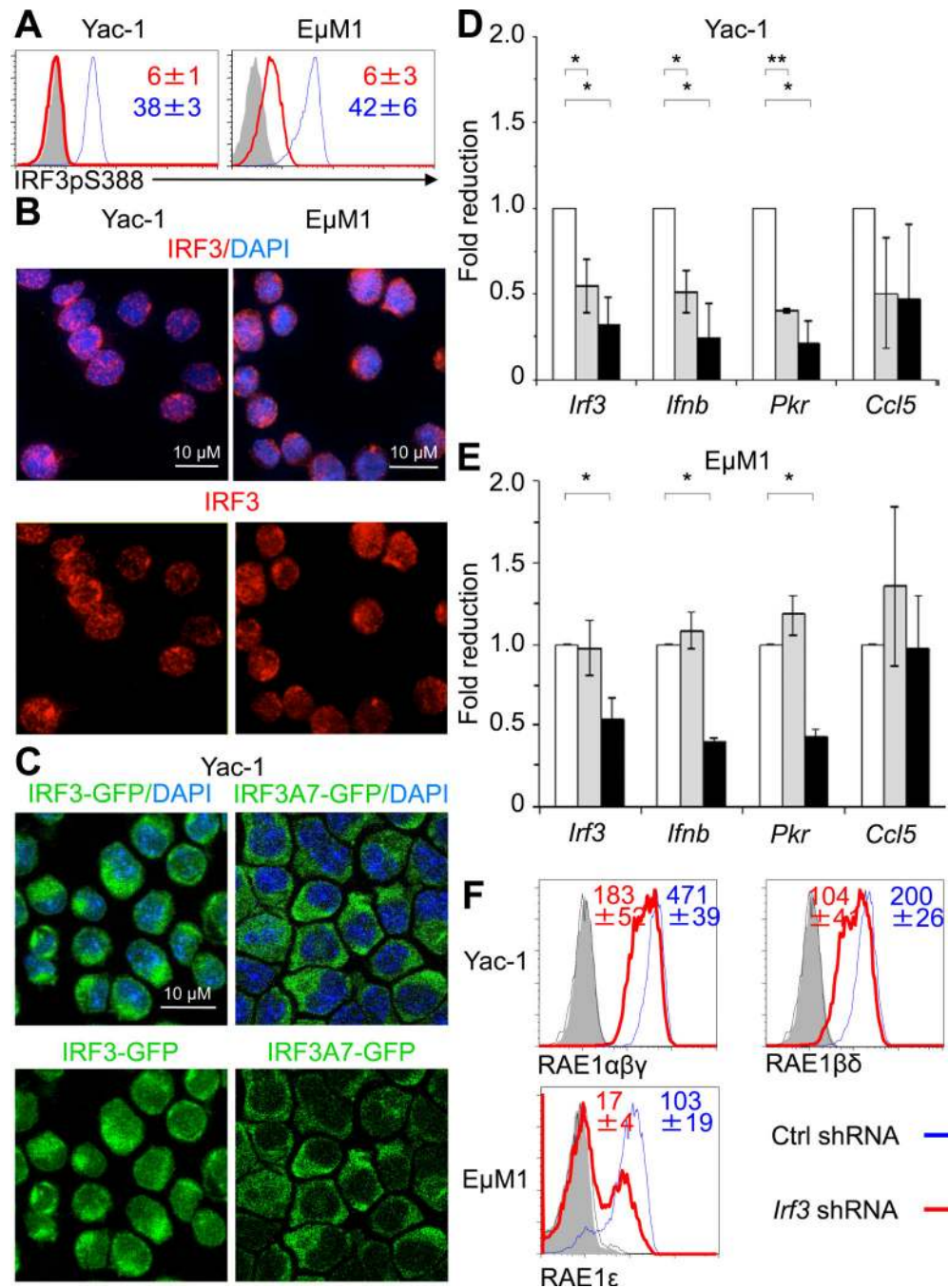
Figure 2. IRF3 is necessary for constitutive RAE1 expression in Yac-1 and EµM1 cells

(A) Expression of IRF3pS388 in Yac-1 and EµM1 was detected by intracellular flow cytometry (blue line). Some cells were pretreated with λ-phosphatase before staining (red line). Filled histogram: isotype-staining of Yac-1 cells. MFI ±SD are indicated. (B) Yac-1 and EµM1 cells were stained for endogenous IRF3 (red) and DAPI (blue). (C) *IRF3-Gfp* or *IRF3A7-Gfp* transduced Yac-1 cells were examined by confocal microscopy for GFP expression in presence of DAPI (blue). (D-E) Relative transcript levels of IRF3 target genes in *Irf3*-specific (grey and black bars) or control shRNAs (white bar)-transduced Yac-1 (D)

and EμM1 (E) cells were analyzed by qRT-PCR. Means ±SD of 3 independent experiments normalized to control shRNA-transduced cells are shown. *p<0.05, **p<0.01. (F) RAE1 expression in *Irf3*-specific (red line) or control (blue line) shRNA-transduced Yac-1 or EμM1 cells 5 days after selection in puromycin. Isotype control staining of *Irf3*- (dotted line) or control shRNA-(filled-histogram) transduced cells is shown. MFI ±SD are indicated.
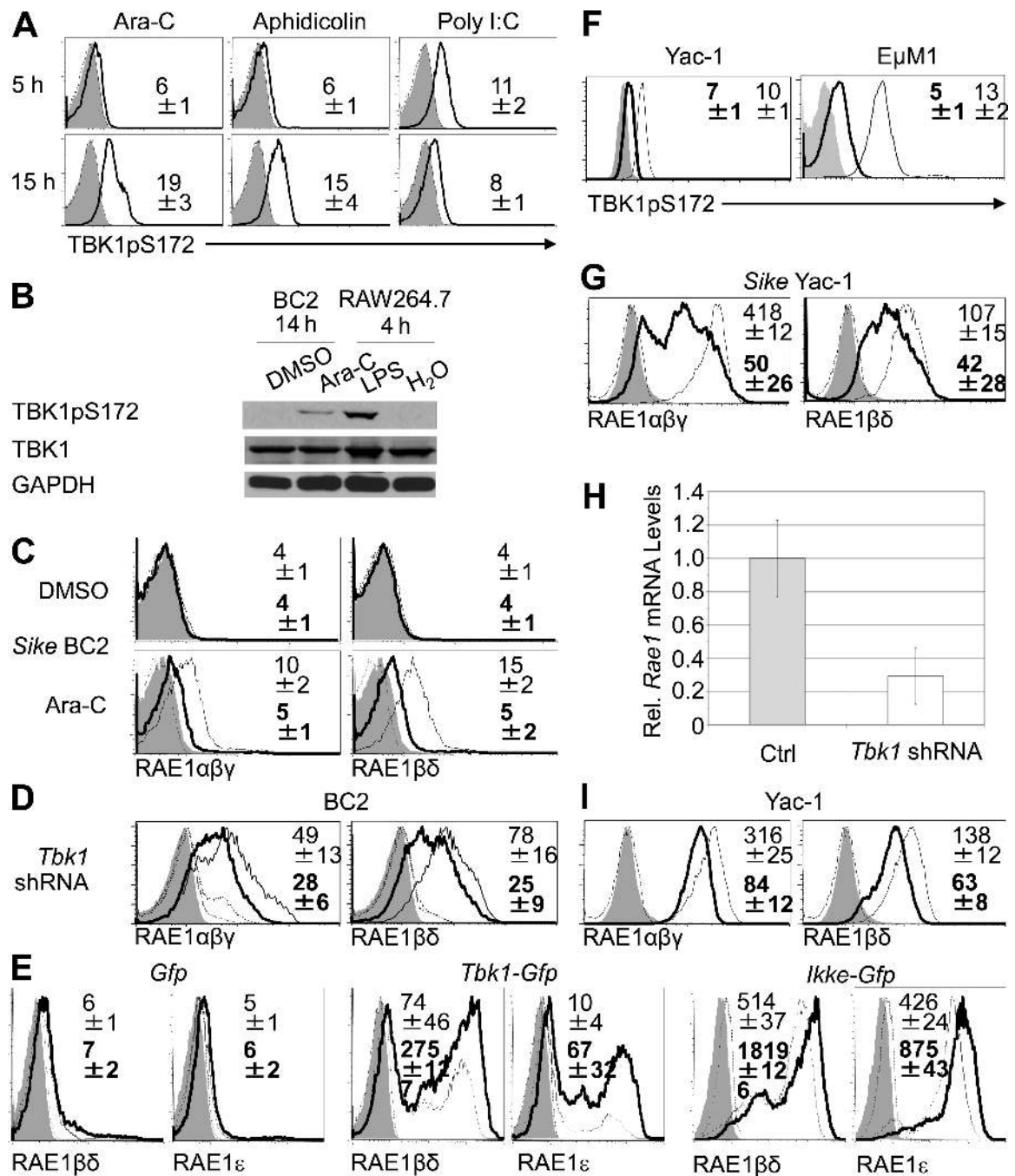
Figure 3. Expression of RAE1 depends on TBK1

(A) Levels of TBK1S172 phosphorylation in BC2 cells treated as indicated in Fig. 1A (bold line) or DMSO (fine line). Filled histograms: isotype staining of DMSO-treated cells. (B) Immunoblot analysis of TBK1S172 phosphorylation in 10 μM Ara-C (14 hrs) or DMSO-treated BC2 cells. Raw 264.7 cells were treated with LPS for 4 hrs for comparison. (C) BC2 cells were transduced with retroviral vectors encoding *Sike* (bold line) or control vector (fine line). 10 days post-transduction BC2 cells were treated with 10 μM Ara-C or DMSO for 16 hrs and stained for RAE1. Isotype staining of control- (dashed line) or *Sike*- (filled

histogram) transduced cells is shown. (D) RAE1 expression in *Tbk1*-specific (bold lines) or control (fine line) shRNA-transduced BC2 cells treated with 10 μM Ara-C for 16 hrs. *Tbk1*-specific (dashed line) or control (dotted line) shRNA-transduced cells treated with DMSO were also stained for RAE1 expression. Filled histogram: isotype control of Ara-C-treated cells. (E) *Tbk1$^{-/-}$Ikke$^{-/-}$* MEFs were transduced with retroviral vectors encoding *Tbk1*, *Ikke* or with empty vector. 8 days after selection, cells were treated with 10 μM Ara-C for 16 hrs (bold line) or DMSO (fine line) and analyzed for the expression of indicated NKG2DLs. Isotype stainings of DMSO (filled histogram) or Ara-C-treated (dashed line) are shown. (F) Levels of TBK1S172 phosphorylation in Yac-1 cells were analyzed by intracellular flow cytometry (fine line). Some cells were pretreated with λ-phosphatase before staining (bold line). Filled histogram: isotype-staining of Yac-1 cells. (G) RAE1 expression in *Sike*-encoding vector (bold line) or empty vector-transduced Yac-1 cells (fine line) 10 days post-transduction. Filled histogram: isotype stainings of *Sike*-expressing cells. Dashed line: isotype control of empty vector-transduced cells. (H) Levels of *Raet1* transcripts were determined by qRT-PCR in *Tbk1*-specific (open bar) or control (filled bar) shRNA-transduced Yac-1 cells 5 days post-transduction. Data represent means ±SD for 3 independent experiments. (I) RAE1 expression in *Tbk1*-specific (bold line) or control (fine line) shRNA-transduced Yac-1 cells. Isotype staining of *Tbk1*-specific (dashed line) and control (filled histogram) shRNA-transduced cells is shown. MFI ±SD are indicated.
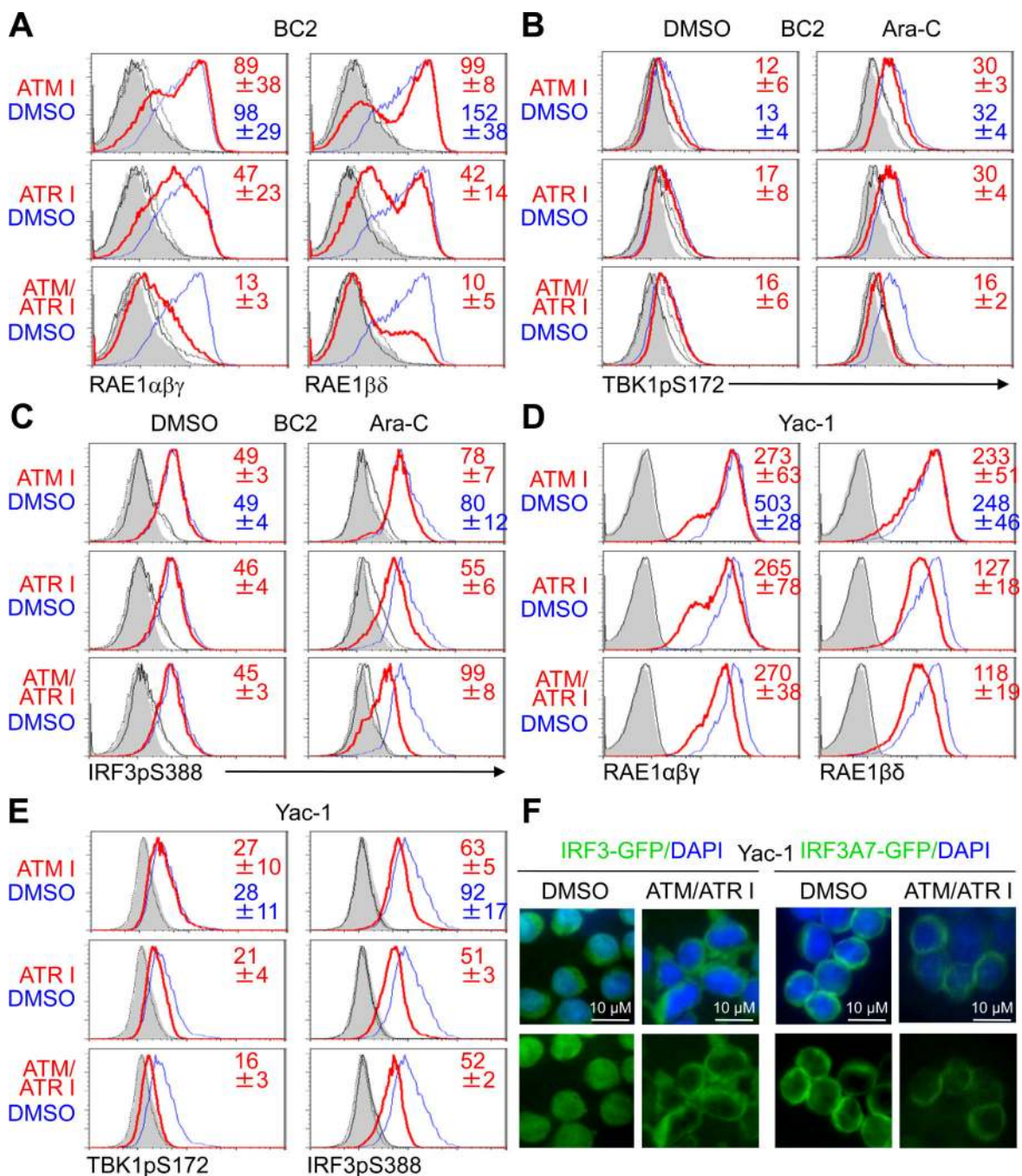
Figure 4. ATR-dependent activation of TBK1 and IRF3 in response to DNA damage
(A-C) Analysis of RAE1 expression (A), phosphorylation of TBK1S172 (B) and IRF3S388
(C) in 10 μM Ara-C-treated (16 hrs) BC2 cells pretreated with 10 μM of the ATM inhibitor
KU55933, the ATR inhibitor VE-821, KU55933+VE-821 (red line) or DMSO (blue line).
Control cells were pretreated with the same inhibitors (dashed line) or DMSO (fine line)
before DMSO treatment. Filled histograms: isotype control staining. MFI ±SD are indicated.
(D-E) Yac-1 cells treated with ATM and/or ATR-specific inhibitors (red line) or DMSO
(blue line) for 16 hrs as indicated above and stained for RAE1 (D), TBK1pS172 (left panel)

and IRF3pS388 (right panel). Filled histograms: isotype control staining. MFI ±SD are indicated (E). (F) *IRF3-Gfp* or *IRF3A7-Gfp*-transduced Yac-1 cells were treated with 10 μM of KU55933+VE-821 or DMSO for 14 hrs. IRF3 expression and DAPI (blue) staining was analyzed by fluorescent microscopy.
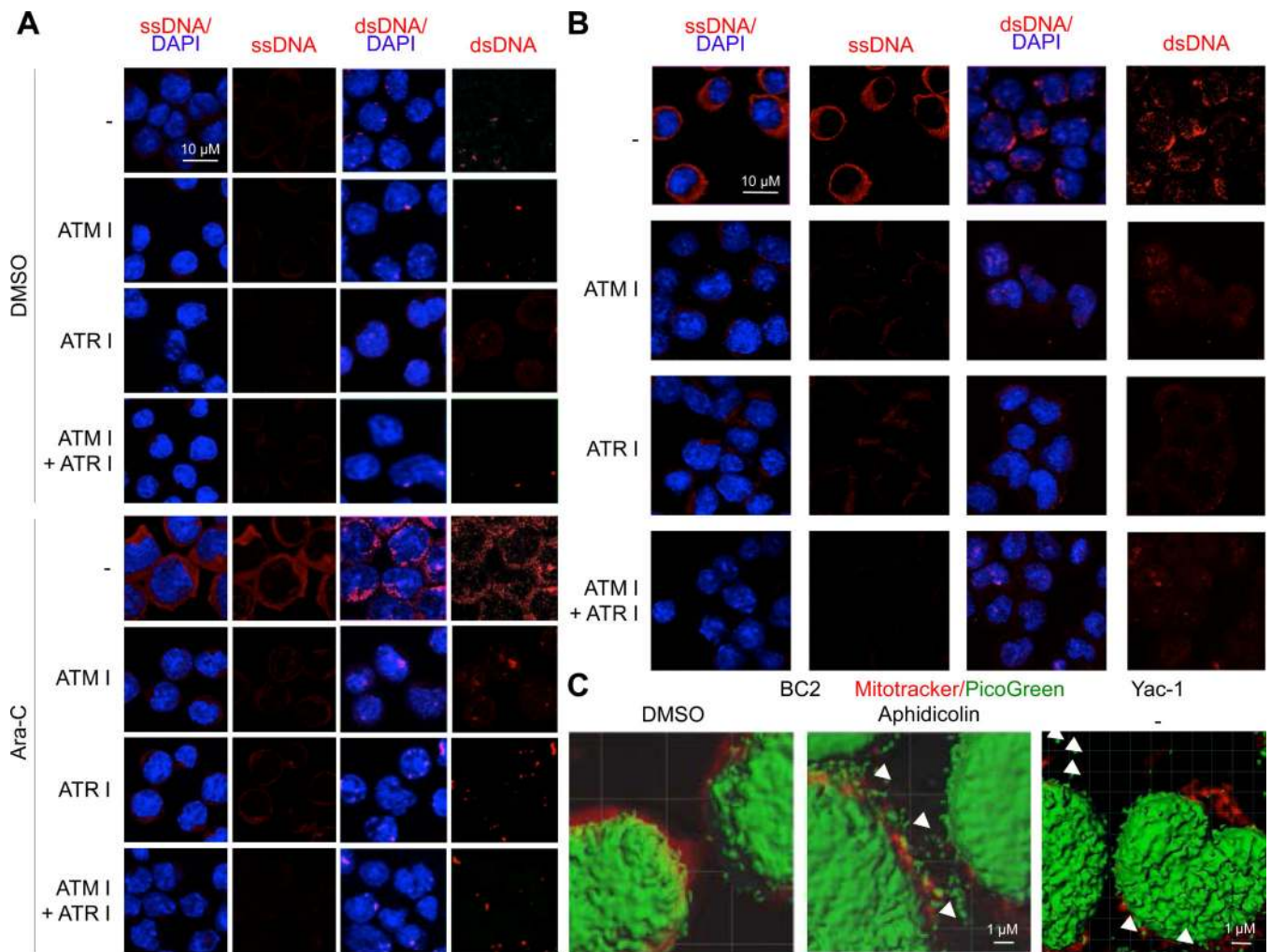
Figure 5. DNA damage leads to the appearance of cytosolic DNA
(A) Staining of BC2 cells for presence of ssDNA (left columns) or dsDNA (right columns) in presence of DAPI (1st and 3rd column). BC2 cells were pretreated with 10 μM of the ATM inhibitor KU55933, the ATR inhibitor VE-821, KU55933+VE-821, or DMSO followed by treatment with DMSO or 10 μM Ara-C for 14 hrs. BC2 cells were treated with RNase and stained with ssDNA- or dsDNA-specific antibodies (red) and DAPI (blue). (B) Yac-1 cells were treated with 10 μM KU55933, VE-821, KU55933+VE-821, or DMSO for 14 hrs and stained as outlined in (A). (C) DMSO (left panel) or 4 μM aphidicolin-treated (middle panel; 14 hrs) BC2 cells and Yac-1 cells (right panel) were incubated with the dsDNA-specific-dye PicoGreen (green) for 1 hr and MitoTracker dye (red) for 15 min. Z-stack images were acquired by confocal microscopy and analyzed using Imaris software to generate iso-surface plots.
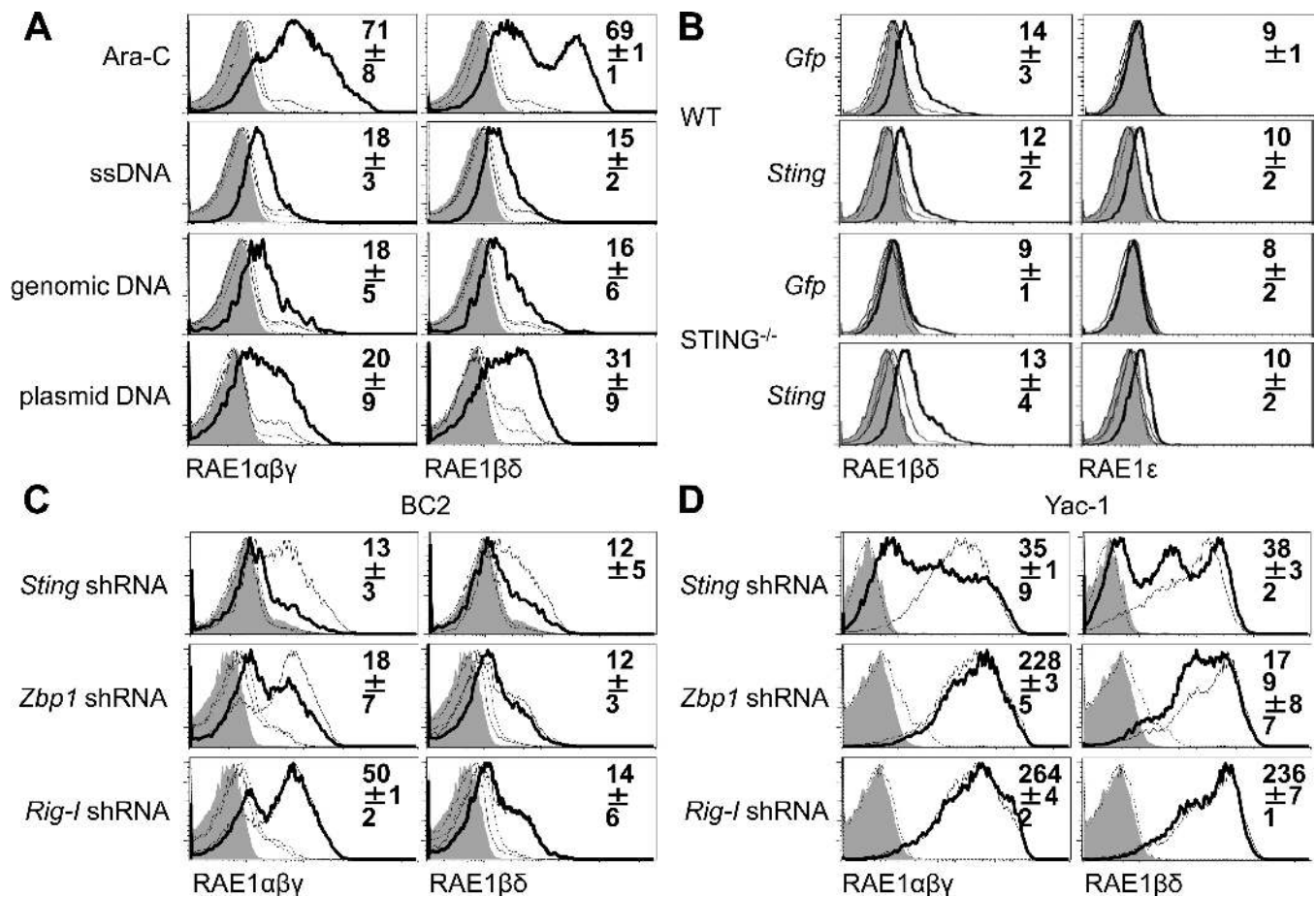
Figure 6. RAE1 expression is induced by cytosolic DNA and depends on STING
(A) BC2 cells were transfected with 4 μg Alexa-488-labelled MSCV-IRES-*Gfp* plasmid DNA, C57BL/6 genomic DNA or ssDNA. Some cells were treated with 10 μM Ara-C or DMSO. 16 hrs later, BC2 cells were stained for indicated NKG2DLs and analyzed by flow cytometry. Bold line: Ara-C-treated or Alexa-488^{+} cells; dashed line: Alexa-488^{−} or DMSO-treated cells; fine line: isotype staining of Ara-C-treated or Alexa-488^{+} cells; dotted line: isotype staining of Alexa-488^{−} cells; filled histograms: isotype staining of DMSO-treated cells. (B) MEFs expressing non-functional or WT *Sting* were transduced with retroviral vectors encoding *Sting* or empty vector. 8 days after selection, cells were treated with 10 μM Ara-C for 16 hrs (bold line) or DMSO (fine line) and stained for indicated NKG2DLs. Isotype stainings of DMSO (filled histogram) or Ara-C-treated cells (dashed line) are shown. (C) *Sting*-, *Zbp1/Dai*- and *Rig-I*-specific (bold line) or control shRNAs-transduced (fine line) BC2 cells were treated with 10 μM Ara-C for 16 hrs. Gene-specific (dashed line) or control shRNA-transduced (dotted line) BC2 cells were also treated with DMSO for 16 hrs. NKG2DL expression was analyzed by flow cytometry. Filled histograms: isotype staining of Ara-treated cells. (D) *Sting*-, *Zbp1/Dai*-, and *Rig-I*-specific (bold lines) or control shRNA-transduced (fine line) Yac-1 cells were stained for NKG2DL expression. Isotype staining of gene-specific (dashed line) or control shRNA (filled histogram)-transduced Yac-1 cells is shown. MFI ±SD are indicated.
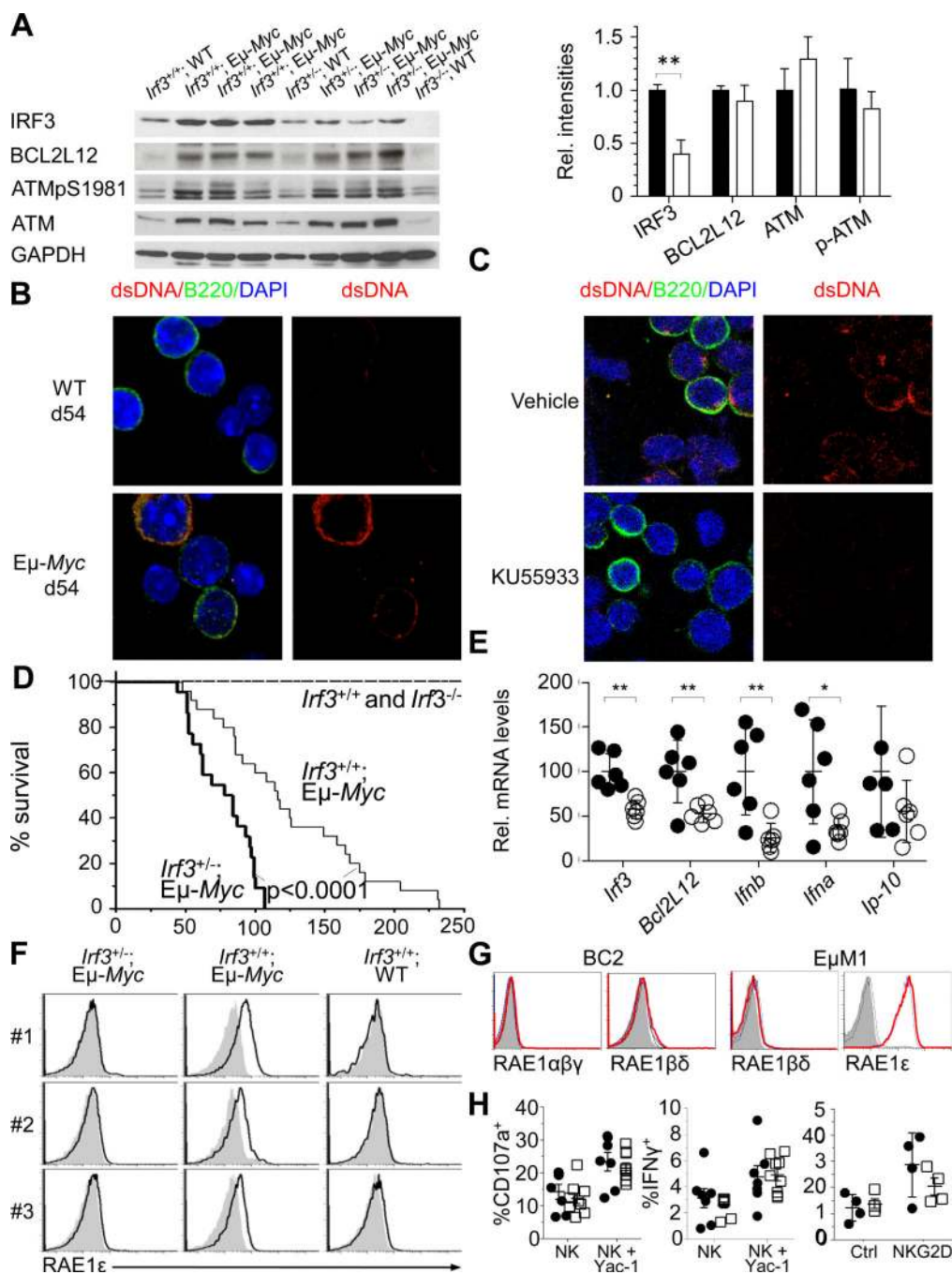
Figure 7. RAE1 Expression in Myc-Driven Lymphomas Depends on IRF3

(A) Immunoblot analysis of splenic B cell lymphomas (>78% purity) from *Irf3*$^{+/-}$;Eμ-*Myc*, Irf3$^{+/+}$;Eμ-*Myc*, *Irf3*$^{+/+}$;WT, *Irf3*$^{+/-}$;WT and *Irf*$^{-/-}$;WT probed with antibodies for IRF3, BCL2L12, ATM, ATMpS1981 and GAPDH (left panel). Densitometry analysis of immunoblots showing mean ±SD from 3 mice normalized to GAPDH levels; **p < 0.01.

(B) B220$^+$ (green) cells of WT and Eμ-*Myc* mice were stained for dsDNA (red) in presence of DAPI (blue) on 54 days of age. (C) Eμ-*Myc* mice were injected i.p. with 5 mg/kg KU55933 (n=3) or vehicle (n=3) on 34 and 36 days of age and stained for dsDNA (red),

B220 (green) and DAPI (blue) on 38 days of age. (D) $Irf3^{+/-}$;Eμ-*Myc* mice (thick) exhibit decreased survival compared to $Irf3^{+/+}$;Eμ-*Myc* (thin line) or non-transgenic (dashed line) or $Irf3^{-/-}$ mice (dotted line). Kaplan-Meier-analysis of survival of $Irf3^{+/+}$;Eμ-*Myc* mice (n=25; median survival=116 days), $Irf3^{+/-}$;Eμ-*Myc* mice (n=17; median survival=62 days) and $Irf3^{+/+}$ or $Irf3^{-/-}$ mice (n=25; median survival= >250 days). p<0.0001 by Log-Rank-Test or by Gehan-Breslow-Wilcoxon-Test. (E) Relative mRNA levels of indicated IRF3 target genes in purified tumor cells of $Irf3^{+/-}$;Eμ-*myc* and $Irf3^{+/+}$;Eμ-*Myc* mice were measured by qRT-PCR. (F) RAE1ε expression in tumor cells of three $Irf3^{+/-}$;Eμ-*Myc* mice. B220^{low} cells in blood of moribund $Irf3^{+/-}$;Eμ-*Myc, Irf3^{+/+}$;Eμ-*Myc* and C57BL/6 mice (bold line) were stained for the indicated NKG2D ligand expression. Filled histogram: isotype staining of B220^{low} tumors. (G) *Bcl2l12*-IRES-*Gfp* (red line) or IRES-*Gfp*-transduced (blue line) BC2 (left panel) or EμM1 (right panel) cells were stained for the indicated NKG2DLs 3 days post-transduction. Dashed line: isotype staining of *Bcl2l12*-IRES-*Gfp*-transduced cells. Fine line: isotype staining of IRES-*Gfp*-transduced cells. Filled histograms: Isotype staining of untransduced cells. (H) IL-2–activated NK cells derived from $Irf3^{+/-}$;Eμ-*Myc* (white squares, n=8) or $Irf3^{+/+}$;Eμ-*Myc* (black circles, n=7) mice were co-cultured with Yac-1 cells at an effector to target ratio of 3:1. After 4 hrs, the percentage of CD107a and IFN-γ-expressing NK1.1$^+$CD3$^-$ cells was determined by flow cytometry (left and middle panel). Freshly isolated splenocytes of $Irf3^{+/-}$;Eμ-*Myc* (white squares, n=4) and $Irf3^{+/+}$;Eμ-*Myc* (black circles, n=4) mice were stimulated *in vitro* for 5 hrs on plates coated with NKG2D-specific antibodies (MI-6, 10 μg/ml), or isotype control (10 μg/ml) before staining and analysis. Intracellular IFN-γ was detected by flow cytometry gated on NK1.1$^+$CD3$^-$ cells (right panel). Error bar denotes standard error of mean.